ACADEMIA ROMÂNĂ
Revue Roumaine de Chimie
https://www.icf.ro/rrch/

Rev. Roum. Chim.,
2023, *68*(10–12), 495–505
DOI: 10.33224/rrch.2023.68.10-12.01

Papers

PREPARATION OF MODIFIED MULTIWALLED CARBON NANOTUBES (L-Arg-CS/MWCNTs-COOH/Fe_3O_4) AS SORBENT FOR DISPERSIVE SOLID PHASE EXTRACTION OF Cu(II), Pb(II) AND Cd(II) IN WASTEWATER SAMPLES

Roghayeh Rais Mohammadi DAHAJI,[a] Ali MOGHIMI,[b,*] Hamidreza SHAHBAZ,[a] Hakim FARAJI[a] and Fariborz AZIZINEJAD[a]

[a]Department of Chemistry, Varamin-Pishva Branch, Islamic Azad University, Varamin, Iran
[b]Department of Chemistry, Faculty of Pharmaceutical Chemistry, Tehran Medical Sciences, Islamic Azad University, Tehran, Iran

Received February 21, 2022

A new modified multiwalled carbon nanotube (l-Arg-CS/MWCNTs-COOH/Fe_3O_4) as sorbent of dispersive solid phase extraction (DSPE) was synthesized for preconcentration and determination of Cu (II), Pb (II), and Cd (II) in wastewater samples. The successful formation of sorbent was characterized by FTIR (Fourier transform infrared) spectroscopy, SEM (Scanning electron microscope), and XRD (X-ray diffraction). Batch experiments such as solution pH, amount of adsorbent, extraction time, type and volume rate of eluent and etc were achieved to study the sorption process. At optimized conditions the adsorbent shows good recovery with 4mL ethylene diamine tetra acetic acid (EDTA) as eluent. Good fitting of sorption kinetics by pseudo-second-order model was obtained. Limits of detection were found in the range of 0.10–0.12 μg L^{-1} for metal ions, the liner range was 5–1000 μg L^{-1} for Cd(II) and 10–1000 μg L^{-1} for Cu(II) and Pb(II) and the preconcentration factor 60, 65 and 55 for Cu(II), Pb(II) and Cd(II), respectively. The relative standard deviation was in the range of 1.5–2.3 %. Results showed that the new magnetic nanosorbent was an efficient DSPE adsorbent for preconcentration and determination of Cu (II), Pb (II), and Cd (II) in wastewater samples.

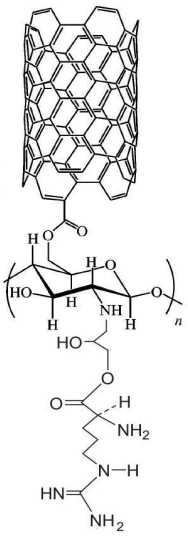

INTRODUCTION

Today, the industrialization of societies pays a heavy price for human beings, especially in the case of environmental water crises,[1,2] One of the water pollutants is related to heavy metals, which, even in small quantities, can cause serious problems in water pollution.[3] Heavy metals can accumulate through the food chain, and eventually enter the human circulatory system and other organisms, threatening their health.[4] Various common methods including adsorption, precipitation, ion exchange, filtration, solvent extraction, and membrane separation have been used to remove heavy

* Corresponding author: kamran9537@yahoo.com; alimoghimi@iauvaramin.ac.ir; ali.moghimi@iaups.ac.ir

metals.[5,6] Solid phase extraction (SPE) is preferred over conventional extraction and preconcentration methods due to low reagent consumption, high speed, cost-effectiveness, high selectivity, and good sensitivity.[7-9] However, magnetic solid phase extraction (MSPE) for extraction and preconcentration of various metal ions has received much attention.[10] In this method, magnetic nanosorbents are easily separated from sample solution by a magnet without centrifugation or sample purification which makes this method faster than SPE.[11]

Since the discovery of carbon nanotubes(CNTs) in 1991, with unique properties such as the above dimension ratio, easy operation, chemical stability and good compatibility have been highly regarded.[12] Functional groups such as hydroxyl and amine are available on CNT as active sites and they also increase the adsorption capacity of metal ions through various mechanisms such as ion exchange, chelation or complexation,[13-15] Raw carbon nanotubes disrupt strong van der Waals interactions in adsorption due to their insolubility and dispersion in all solvents,[12] Chemical modification of CNT can increase dispersibility and also improve the metal adsorption and selection in SPE,[16-18] Chitosan is a natural polymer with many properties such as good abundance, low cost, non-toxicity and biocompatibility.[19] Through the alkaline distillation of chitin, which is the main component of crab, shrimp and krill shells, it is produced and supplied at a low price.[20,21] Chitosan is a suitable polymer to modify CNTs for wastewater treatment.[22-25] Also, compounds containing oxygen, nitrogen and sulfur have been used extensively to remove the limitation of chitosan adsorption capacity and its surface modification.[3]

In this work, a new magnetic nanosorbent was synthesized as an adsorbent for dispersive solid phase extraction(DSPE) to shorten the time of sample preparation and also facilitated the separation of Cu(II), Pb(II) and Cd(II) in industrial wastewater samples and then determination by flame atomic absorption spectroscopy(FAAS).

Modification of nanotubes by chitosan has already been studied, *e.g.*, by Tang *et al.*, [26] but in this work, by binding l-Arginin (l-Arg) (which is a biocompatibility and low cost amino acid) to chitosan, the functional groups(–COOH, $–NH_2$ and –NH–) for the adsorption of metal ions were increased, and also because of the magnetism of the adsorbent, the separation was very simple and fast.

The synthesized magnetic nanosorbent was characterized by SEM, XRD and FT-IR and it was found the investigated method was good for preconcentration and determination of target metal ions in industrial wastewater samples.

EXPERIMENTAL

1. Reagents and materials

Chitosan (deacetylation rate > 90%) was purchased from Sigma-Aldrich (Darmstadt, Germany). A Carboxylated multiwalled carbon nanotube (MWCCNT) was obtained from Sigma-Aldrich (Darmstadt, Germany. Solutions of Cu(II), Pb(II) and Cd(II) were prepared individually by dissolving an appropriate amount of the ($Pb(NO_3)_2$), ($Cu(NO_3)_2.3H_2O$) and ($Cd(NO_3)_2$) by purity > 99.5% (Merck (Darmstadt, Germany) in 1% HNO_3 and mix working solution was prepared by Step by step dilution of the stock solutions. Glutaraldehyde 25% (purity > 99.5%) and ethylene diamine tetra acetic acid (EDTA) (purity > 99.5%), l-Arginine (purity > 99%) were prepared from Merck (Darmstadt, Germany). 2 ml of 1.0 mol L^{-1} acetate buffer was added to adjust the pH of the solutions.

2. Instruments

The Fourier transform infrared (FTIR) spectra were recorded in the range 4000–400 cm^{-1} using the KBr pellet technique (Thermo, AVATAR, Massachusetts, USA). A supermagnet with 1.2 T magnetic field, N35 model from Tehran Magnet (Tehran, Iran) was used for magnetic separation. A flame atomic absorption spectrometer (FAAS) (Varian Spectra AA 200, Australia) was applied to determination of metal ions. A scanning electron microscope (SEM, PHILIPS, CM120, Amsterdam, Netherlands) was used for the surface morphology of the nanosorbent.

3. Synthesis of the magnetic nano sorbent

3.1. Synthesis of the Fe_3O_4 /MWCNTs-COOH composite

0.08 g of $FeCl_2$ and 0.216 g of $Fecl_3$ were dissolved in 200 mL of deionized (DI) water. 0.04 g of MWCNTs-COOH was added to the homogeneous mixture and heated to 50°C for 20 min under the N_2 atmosphere. After cooling, the black mixture was dispersed in ultrasound for 20 min. 1.0 mL NH_3 was added to previous solution and heated to 50 °C for 40 min under the N_2 atmosphere. The solution was washed three times with DI water and the solution was separated from the precipitate by a magnet and dried in a vacuum oven at 80°C.

3.2. Synthesis of the l-Arg-CS

1.0 g CS powders were dissolved in100 mL aqueous acetic acid solution (2.0%, v/v). 100 mL NaOH 0.25 mol L^{-1} was added to the previous stirring solution. After precipitation the product was washed with acetone and suspended in 100 mL acetone. 5 mL epoxy chloropropane was added to the above suspension and stirred continuously at 25 °C for 24 h. 2.00 g l-Arg dissolved in 40 mL DI water and was added into the above solution system and refluxed for 7 h at 50 °C. Then 0.25 g l-Arg dissolved in 10 mL DI water. Then, 30 mL NaOH 1.00 mol L^{-1} and 0.05 g KI were added, and the mixture was stirred for 5 h. The product was

cooled, washed with DI water and acetone. Finally, the residue was dried in a vacuum oven at 50 °C.

3.3. Synthesis of the l-Arg-CS/MWCNTs-COOH/Fe3O4

1.0 g of l-Arg-CS, 1.0 g of Fe_3O_4 /MWCNTs-COOH, and 0.4 mL glutaraldehyde were dissolved in 400 mL of acetic acid(2.0%, v/v) and mixed for 40 min at 40 °C under the N_2 atmosphere. Then 1.0 L DI water and 120 mL of 0.10M NaOH were added to the mixture and stirred for 30 min under the N_2 atmosphere. After cooling the solution, the water was removed from the sponge-like mixture with a pipette. The magnetic nanosorbent was dried at 80 °C in a vacuum oven for 12 h and powdered. Scheme 1, shows the form of the adsorbent.

4. Preconcentration procedure experiments

Typically, 10 mg of the nanosorbent was added to 100 mL of the mixed metal ions solution in a 150 mL flask and the pH was adjusted to 6 with buffer solution, stirred for 6 min by mechanical stirring, and then the solid phase was separated with a magnet. The metal ions were desorbed with 4 mL of EDTA for 5 min before determination by atomic absorption spectrometry. All the experiments were performed 3 times.

The adsorption % was calculated by equation (1):

$$R\% = \left({}^{(C_i - C_f)}/_{C_i} \times 100 \right) \quad (1)$$

where C_i is the initial concentration of metal ion in mg L^{-1} and C_f is metal ion concentration (mg L^{-1}) after adsorption.[9, 27]

RESULTS AND DISCUSSION

1. Characterization

1.1. IR spectra analysis

The FTIR spectra of Fe_3O_4 /MWCNTs-COOH, l-Arg-CS, l-Arg-CS/MWCNTs-COOH/Fe_3O_4 and l-Arg-CS/MWCNTs-COOH/Fe_3O_4-Cu are shown in Fig. 1.

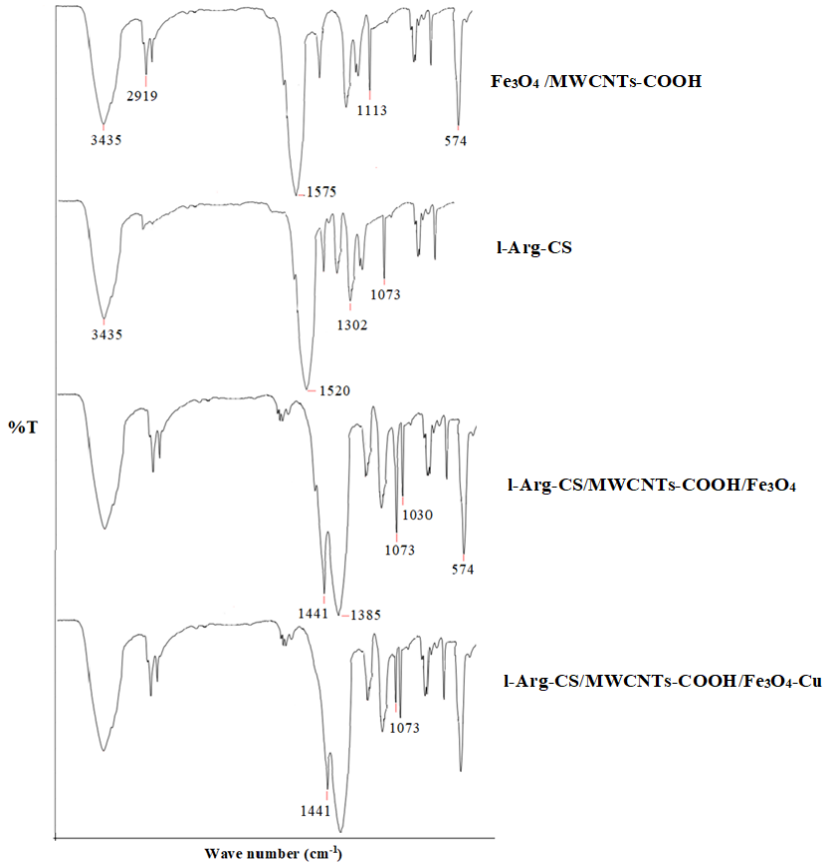

Fig. 1– FT-IR spectra of Fe_3O_4 /MWCNTs-COOH, l-Arg-CS, l-Arg-CS/MWCNTs-COOH/Fe_3O_4 and l-Arg-CS/MWCNTs-COOH/Fe_3O_4-Cu.

In Fe_3O_4/MWCNTs-COOH spectrum, the stretching vibrations at 3435 cm^{-1}, 2919 cm^{-1}, 1575 cm^{-1}, 1113 cm^{-1} and 574 cm^{-1} can be related to the stretching vibration of hydroxyl, aliphatic O–H, C–H, –C–O, C– O and Fe–O, respectively.[24-29] In l-Arg-CS spectrum, peaks in areas 1520 cm^{-1} and 1302cm^{-1} may be related to asymmetry and symmetry stretching vibration of –COO– in l-Arg. The peak at 1073 cm^{-1} assigned to the stretching vibration of –C–N. In fact, it was the reaction between –Cl and $–NH_2$.[3] The peak at 1441 cm^{-1} in FTIR spectra of l-Arg-CS/MWCNTs-

COOH/Fe_3O_4 can be attributed to N–H bending vibration of amino. Two peaks at 1385 cm^{-1} and 1030 cm^{-1} are probably related to C– O and the bridge between OH of the CS and C–O–C groups, respectively.[24] Probably, decreased the intensity of peaks at 1441 cm^{-1} and 1073 cm^{-1} in the l-Arg-CS/MWCNTs-COOH/Fe_3O_4-Cu spectrum was to the involvement of active sites for adsorbed of Cu(II).[11] Finally, results showed that successful adsorption of metal ions on the l-Arg-CS/MWCNTs-COOH/Fe_3O_4.

1.2. XRD analysis

Figure 2 depicts the XRD curves of CS, Fe_3O_4 /MWCNTs-COOH and l-Arg-CS/MWCNTs-COOH/Fe_3O_4. In the XRD pattern of CS, two peaks were observed at 2θ = 10º and 20º. In XRD pattern of Fe_3O_4 /MWCNTs-COOH, the peak at 2θ = 26º confirms the existence of MWCNTs and Five peaks at 2θ=30.1º, 35.5º, 43.3º, 57.2º, & 62.5º related the diffraction peaks of Fe_3O_4.[10,19] In curves of l-Arg-CS/MWCNTs-COOH/Fe_3O_4 the diffraction peaks of CS due to decreasing in crystallinity were decreased and all the peaks related to Fe_3O_4 were observed. Also, intensity change in MWCNTs peak demonstrates the grafting of l-Arg-CS on MWCNTs- COOH.[1,11] The results confirm the successful modification of MWCNTs-COOH.

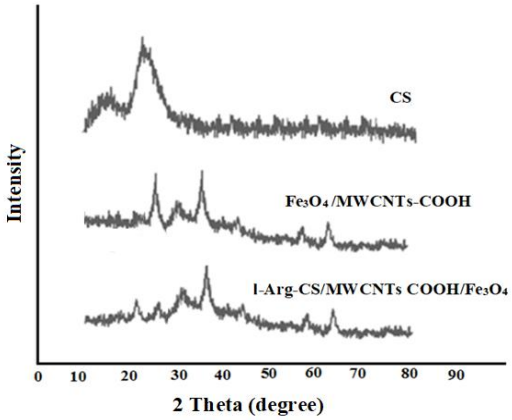

Fig. 2 – XRD curves of CS, Fe_3O_4 /MWCNTs-COOH and l-Arg-CS/MWCNTs COOH/Fe_3O_4

1.3. SEM images

The SEM images in Fig. 3 have explored the surface morphology and determined the size of MWCNTs-COOH/Fe_3O_4 and l-Arg-CS/MWCNTs-COOH/Fe_3O_4. The size of MWCNTs COOH/Fe_3O_4 was in the range of 11–15 nm and the size of l-Arg-CS/MWCNTs-COOH/Fe_3O_4 was in the range of 11–24 nm. Brighter spots in the SEM image of l-Arg-CS/MWCNTs-COOH/Fe_3O_4 probably indicate the modification of MWCNTs-COOH/Fe_3O_4 with l-Arg-CS or in other words related to the interaction between carboxylic acid and chitosan.

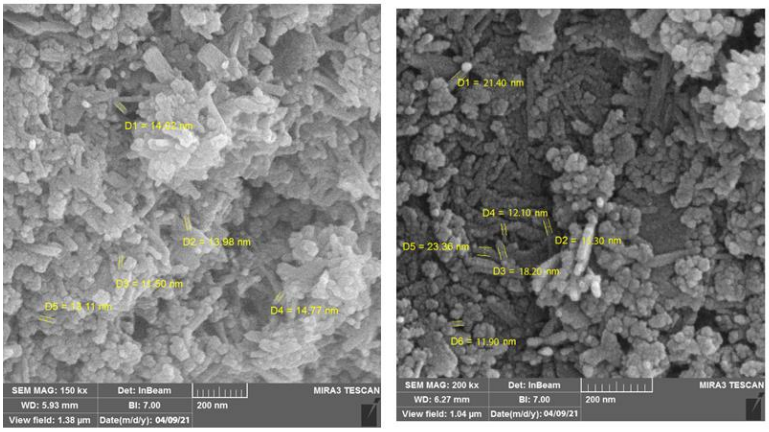

Fe3O4 /MWCNTs-COOH l-Arg-CS/MWCNTs-COOH/Fe3O4

Fig. 3 – SEM photographs of Fe_3O_4 /MWCNTs-COOH and l-Arg-CS/MWCNTs-COOH/Fe_3O_4.

2. Optimization of the proposed method variables

2.1. Effect of pH

The pH of the solution plays an important role in the solubility of the metal ions and the surface adsorbent charges.[10] The pH of the solutions was adjusted with buffer solutions and was investigated in the range of 0.2–0.8. The pH above 8 has not been investigated due to metal ions precipitation and leads to a false change of adsorption.[11] The results showed that at first by increasing pH, the relative recoveries increased and finally decreased at higher pH values (Fig. 4a). In the low value of pH, the protonation degree was reduced. Consequently, the interaction between the metal ions and the binding site is enhanced. In higher pH (pH > 6), a decrease in the relative recoveries may be due to the hydrolysis of metal ions and the formation of metals hydroxide.[25] Therefore, the pH = 6, was chosen for optimum pH in the metal ion solutions. Similar results were previously reported by Salehi *et al*.[11]

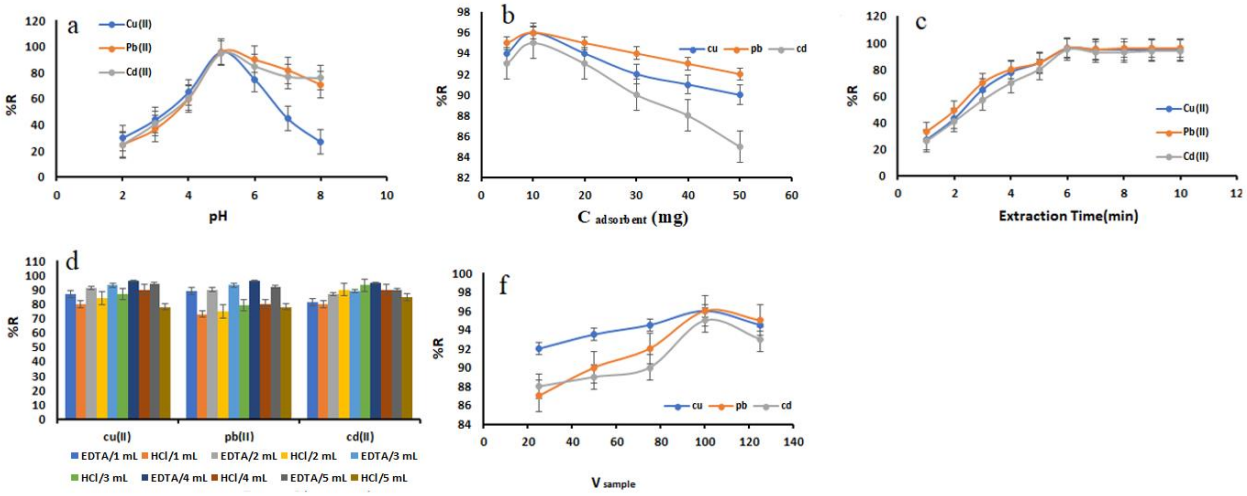

Fig. 4 – a) Effect of pH; b) dosage of adsorbent (mg); c) extraction time (min); d) type and volume of eluent; f) sample volume (mL). Experimental parameters: in b, c, d and f pH = 5, C_e(M) = 0.5 ppm; wt of MG-Chi/Fe_3O_4= 10 mg in a, c, d and f. Extraction time = 6 min in a, b, d and f ; type and volume of eluent = 4mL EDTA in a, b, c and f; sample volume =100 mL in a, b, c and d.

2.2. Effect of the adsorbent dose

The adsorbent dosage was investigated in the range of 5–30 mg in 100 mL of sample solution. The relative recoveries increased at first with increasing the adsorbent dosage and then it was almost constant after 10 mg (Fig. 4b). This increase in relative recoveries may be due to an increase in adsorption sites, and once the adsorption equilibrium is reached, a large number of adsorption sites will reduce adsorption.[25]

2.3. Effect of extraction time

The Effect of extraction time was determined by measuring relative recoveries at 1–10 min (Fig. 4c). As the extraction time increases, the adsorption increases due to the increase in the active sites until the adsorption reaches equilibrium and then remains constant, possibly due to the repulsion between the adsorbed metal ions and the sample solution. The most relative recovery occurred within 6 minutes of extraction time.[19]

2.4. Effect of type and volume rate of eluent

1–5 mL of hydrochloric acid (HCl) 0.5 and 4 mL EDTA with 5 min contact time were investigated to achieve high preconcentration factors. The results demonstrated that 4mL EDTA causes the maximum relative recoveries (Fig. 4d).

2.5. Effect of sample volume

To determine the enrichment factor, the maximum sample volume at which the adsorption efficiency is maximum was measured. The removal efficiency decreased if the sample volume increased more than 100 ml (Fig. 4f). This was probably due to the decrease in contact between the metal ions and active sites on the magnetic nanosorbent.[11]

2.6. Effect of interfering ions

For the study of the effect of interfering ions on the ability of the magnetic nanosorbent some

cations and anions in varying concentrations were investigated. Effect of interfering ions plays very important role in making a determination error.[11] The results showed that interfering ions had insignificant interference the extraction and determination of metal ions (Table 1).

Table 1

Effect of interfering ions on the determination of metal ions

%Recovery			$C_{\text{interfering ion}}/C_{\text{metal ions}}$	interfering ion
Cd(II)	Pb(II)	Cu(II)		
98	96	98	100	Cr^{3+}
98	98	96	100	Cr^{5+}
96	97	96	50	Na^{+}
98	98	97	50	Ca^{2+}
97	98	95	50	Ni^{2+}
98	96	98	100	Nitrite
96	98	97	100	Nitrate

$n = 3$

3. Adsorption kinetics

One critical parameters for evaluating the sorption performance is the sorption speed. Therefore, three kinetic models such as pseudo-first-order, pseudo-second-order and intraparticle diffusion were used to investigate the rate of the adsorption process.[26]

Linear forms of these equations are represented in equations (2), (3) and (4), respectively:[11, 30-32]

$$1/q_t = \left(K_1/q_e t\right) + \left(1/q_e\right) \quad (2)$$

$$t/q_t = \left(1/K_2 q_e^2\right) + \left(t/q_e\right) \quad (3)$$

$$q_t = K_P t^{1/2} + C \quad (4)$$

where q_t (mg g^{-1}) and q_e (mg g^{-1}) are the adsorption capacities of metal ions at time t (min) and equilibrium time (min), respectively, while k_1 (min^{-1}), k_2 (g mg^{-1} min^{-1}) and k_p (mmol $g^{-1}min^{1/2}$) are the pseudo-first-order, pseudo-second-order rate and intraparticle diffusion constants, respectively.

After comparing the values obtained using pseudo-first-order and pseudo-second-order models, it is evident that the adsorption kinetics of metal ions on magnetic nanosorbent are more consistent with the pseudo-second-order model. The results of the tables and graphs (Tables 2 and Figs. 5a and 5b) confirm that the rate limiting step is chemisorption comprising the interaction of charges between metal ions and magnetic nanosorbent. Also, the obtained results in Table 1 and Fig. 5c showed that the R^2 was a bad agreement with the experimental data and the intraparticle diffusion was not the only rate limiting step and the inner-diffusion resistance was not significant to control the adsorption of metal ions.[19, 33]

Table 2

Parameters of kinetic model for the sorption metal ions

	q_e (mg g^{-1})	k_1 (min^{-1})	R^2	q_e (mg g^{-1})	k_2 (g(mg $min)^{-1}$)	R^2	K_P (mmol $g^{-1}min^{1/2}$)	C	R^2
Cu(II)	60.26	20.12	0.9752	55.65	1.81×10^{-3}	0.9915	4.2632	18.125	0.7625
Pb(II)	60.32	17.34	0.9658	57.66	1.79×10^{-3}	0.9925	4.5265	20.189	0.7764
Cd(II)	59.45	21.22	0.9782	54.89	1.75×10^{-3}	0.9905	4.6258	17.205	0.7518

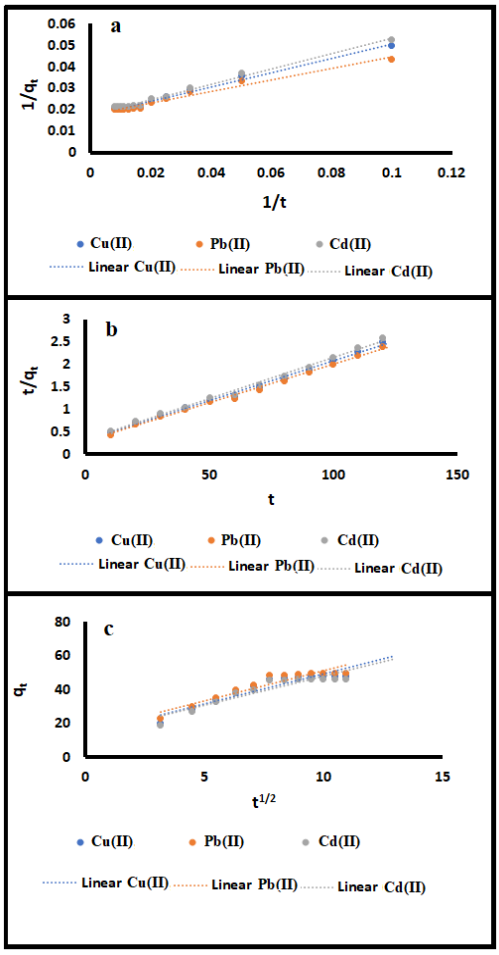

Fig. 5 – a) Pseudo first order kinetic model; b) pseudo second order kinetic model; c) intraparticle diffusion model for the adsorbtion of metal ions.

4. Reusability of l-Arg-CS/MWCNTs-COOH/Fe_3O_4

To evaluate the potential of the adsorbent on a large scale, reduce the overall cost and the possibility of recovering metals extracted from the aqueous solution; it is necessary to measure the ability of the adsorbent to desorb particles.[34] The result in Fig. 6 showed that the relative recovery was still good after six adsorption-desorption cycles. This can be attributed to the effect of 4 mL of EDTA, which is a strong chelating agent.[11]

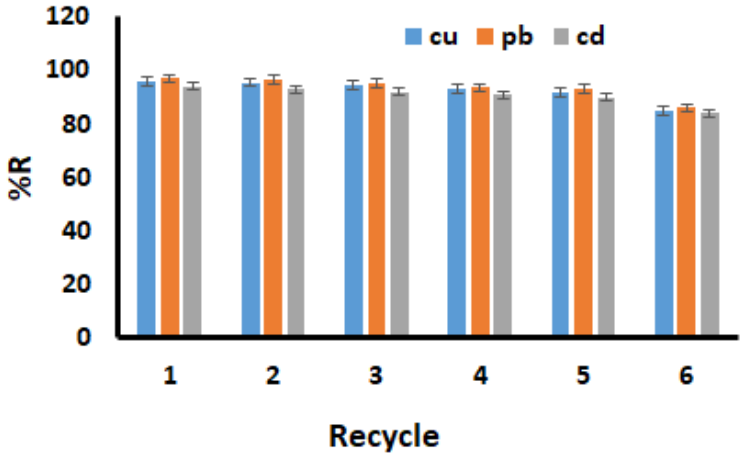

Fig. 6 – Reusability of l-Arg-CS/MWCNTs COOH/Fe_3O_4.

5. Validation of the method

The results and analytical performance were summarized in Table 3 for the proposed method under the optimized conditions. The coefficient of determination (r^2) for all metal ions was above 0.99 (Fig. 7).

Table 3

Analytical figures of merit for the determination of metal ions

R^2	%E	LDR (µg L^{-1})	EF	%RSD (n = 3)		LOQ (µg L^{-1})	LOD (µg L^{-1})	Metal ion
				Interday	Intraday			
0.9983	115	10-1000	60	1.8	2.3	10	0.12	**Cu(II)**
0.9979	125	10-1000	65	3.5	2.8	10	0.12	**Pb(II)**
0.9984	110	5-1000	55	3.0	1.5	5	0.10	**Cd(II)**

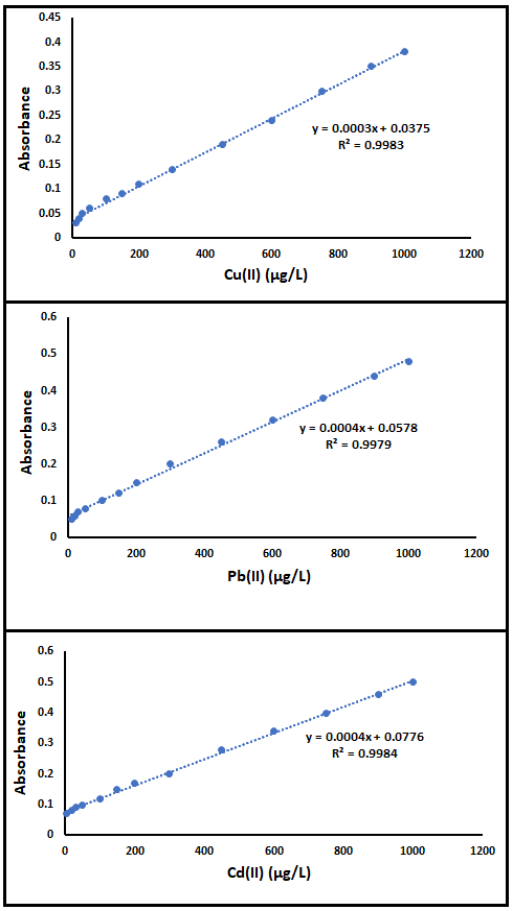

Fig. 7 – Calibration curve of the proposed method for metal ions.

The limit of detection (LOD) was calculated according to the following equation:

$$\mathbf{LOD} = {}^{3\mathrm{SD}}/_{\mathrm{m}} \qquad (5)$$

where SD is the standard deviation of 10 consecutive measurements of blank solutions and m is the slope of the calibration curves.[34] Also, the limit of quantification and Linearity were showed. Both RSDs of intraday and interday were calculated and were demonstrated good precision. Preconcentration factor (PF) was calculated according to the equation shown below:[35]

$$PF = {}^{C_1}/_{C_0} \quad (6)$$

C_1 is the concentration of the analyte in the solid phase and C_0 is the initial concentration of the analyte. And also Extraction percentage (%E) calculated and shown for all metal ions.

6. Real samples analysis

Real samples were collected in a clean glass bottle from the SAIPA Company's wastewater (Tehran, June, 2021, pH = 8, Temp = 298 K). Then they were filtered with a membrane filter with a pore size of 0.45 μm. Under the optimum conditions, the real samples and spiked wastewater samples with two levels of concentration of Cu(II), Pb(II) and Cd(II), RSDs for 3 replicate measurements were in the range of 1.5–2.8%. And then relative recoveries (R%) were evaluated and were above 100. All results that were reported in Table 4 and the accuracy of the developed method demonstrated this method was good efficient for the preconcentration and determination of metal ions from wastewater samples.

Table 4

Determination of metal ions in the SAIPA's wastewater sample

%R	RSD (n = 3)	C determined (μg L^{-1})	C added (μg L^{-1})	Metal ion
103	1.4	50.19	50	**Cu(II)**
102	1.8	100.25	100	
103	2.3	51.26	50	**Pb(II)**
101	1.4	100.56	100	
104	1.5	51.00	50	**Cd(II)**
103	1.8	100.50	100	

7. Comparison of the developed method with previously reported methods

LOD, extraction time and recovery, are an important factors in the adsorbed of metal ions. Therefore these factors were compared with previously reported methods for the adsorption of metal ions in Table 5.[25,36-39] The results indicated that the recovery of the present method was better than the previous methods. In addition, the extraction time was shorter than reported methods for the simultaneous determination of metal ions and the LODs were good. So, the l-Arg-CS/MWCNTs-COOH/Fe_3O_4 as an adsorbent for the proposed method was successfully applied for preconcentration and determination of metal ions.

Table 5

Comparison of the proposed method with some of the methods reported in the literature for determination of the metal ions

Metal ion	Adsorbent	LOD (μg L^{-1})	Extraction time (min)	%Recovery	Ref.
Pb(II)	Fe3O4@Z-NCNT/PC	*	20	>98%	[25]
Cd(II) Pb(II)	MWCNTs	0.001 0.03	120 120	103 102	[36]
Pb(II)	modified multiwalled carbon nanotubes	0.26	10	97	[37]
Cu(II)	MWCNT-Bi_2S_3 nanomaterial	3.98	2	92-100	[38]
Cd(II) Cu(II) Pb(II)	magnetic allylamine MWCNTs-TB	0.00056 0.00022 0.00018	15 15 15	98-102 98-102 98-102	[39]
Cu(II) Pb(II) Cd(II)	l-Arg-CS/MWCNTs-COOH/Fe_3O_4	0.12 0.12 0.10	6 6 6	103 103 104	This work

*Not report

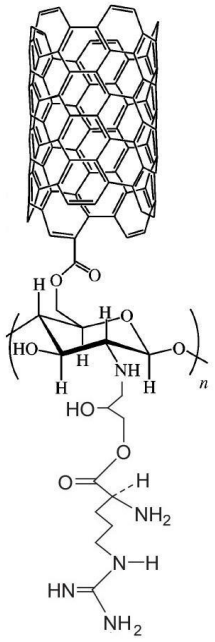

Scheme 1 – The form of the l-Arg-CS/MWCNTs COOH/Fe_3O_4.

CONCLUSION

In this work, we have synthesized a new magnetic nanosorbent as a sorbent for preconcentration and determination of metal ions from wastewater samples and then characterized by FT-IR, SEM and XRD. Good preconcentration factors were obtained that showed the efficiency of the synthesized sorbent. The sorption kinetics could be described by the pseudo-second-order model. The desorption analysis demonstrated this sorbent can be reused for 5 cycles of adsorption and it was very rapid separation by a magnet. Finally, this validated method was applied for the preconcentration and determination of metal ions from wastewater samples.

REFERENCES

1. S. R. Mousavi, M. Asghari and N. M. Mahmoodi, *Carbohydr. Polym*., **2020**, *237*, 116–128.
2. A. Moghimi, *Chin. J. Chem. Soc.* **2008**, *55*, 369–376.
3. T. Pourshamsi, F. Amri and M. Abniki, *J. Iran. Chem. Soc.*, **2021**, *18*, 245–264.
4. X. Wang, Q. Fan, S. Yu, Z. Chen, Y. Ai, Y. Sun, A. Hobiny and A. Alsaedi, *Chem. Eng. J.*, **2016**, *287*, 448–455.
5. M. Abniki, Z. Azizi, S. Poorebrahim and E. Moniri, *Biomed. Phys. Engineering Express*, **2023**, *9*, 045021.
6. M. Abniki, A. Moghimi and F. Azizinejad, *J. Serbian Chem. Soc.*, **2020**, *85*, 1223–1235.
7. M. Abniki, A. Moghimi and F. Azizinejad, *J. Chinese Chem. Soc*., **2021**, *68*, 343–352.
8. A. Moghimi and M. Abniki, *Chem. Methodol*., **2021,** *5*, 250–258.
9. A. Moghimi and M. Abniki, *Adv. J. Chem. Sect. A.*, **2021**, *4*, 78–86.
10. F. Sharifianjazi, A. J. Rad, A. Bakhtiari, F. Niazvand, A. Esmaeilkhanian, L. Bazli, M. Abniki, M. Irani and A. Moghanian, *Biomedical Materials*, **2021**, *17*, 012002.
11. N. Salehi, A. Moghimi and H. Shahbazi, *IET Nanobiotechnol.*, **2020**. DOI: 10.1049/nbt2.12025.
12. R. Sitko, B. Zawisza and E. Malicka, *Trends Anal. Chem*., **2012,** *37*, 22–31.
13. A. Moghimi and N. Tajodini, *Asian J. Chem*., **2010**, *22*, 3325–3334.
14. J. Kathi, K. Y. Rhee and J. H. Lee, *Compos. Pt. A. Appl. Sci. Manuf*., **2009**, *40*, 800–809.
15. Z. Huang, Z. Li, L. Zheng, L. Zhou, Z. Chai, X. Wang and W. Shi, *Chem. Eng. J.*, **2017**, *328*, 1066–1074.
16. Y. P. Sun, K. Fu, Y. Lin and W. Huang, *Acc. Chem. Res*., **2002**, *35*, 1096–1102.
17. M. Burghard and K. Balasubramanian, *Small.*, **2004**, *1*, 180.
18. N. Tajodini and A. Moghimi, *Asian J. Chem*., **2010**, *22*, 3335–3344.
19. N. Salehi, A. Moghimi and H. Shahbazi, *Int. J. Environ. Anal. Chem*., **2020**. DOI: 10.1080/03067319.2020.1753718.
20. N. N. Safie, A. Z. Yaser and N. Hilal, *Asia-Pac. J. Chem. Eng*., **2020**, *15*, 2448–2456.
21. O. Silva, J. E. Francisco, J. C. M. Cajé, R. J. Cassella and W. F. Pacheco, *J. Environ. Sci. Health A.*, **2017**, *53*, 55–64.
22. M. Abniki, Z. Azizi and H. A. Panahi, *IET nanobiotechnology*, **2021**, *15*, 664–673.
23. A. Moghimi, M. Shojai and M. Abniki, *J. Qquantum Chem. Spectroscopy*, **2021,** *11*, 55–43.
24. M. Abniki, B. Shirkavand Hadavand, F. Najafi and I. Ghasedi, *J. Macromolec. Sci.*, Part A, **2022**, *59*, 411–420.
25. B. Shirkavand, M. Abniki, Z. Rahmani, R. Esmaili Salmi and P. Rezaei Behbahani, *J. Textile Sci. Technol.*, **2023**, *12*, 17–26.
26. M. Soylak and R. Maulana, *Int. J. Environ. Anal. Chem.*, **2023**, *103*, 2542–2554.
27. R. Motallebi, A. Moghimi, H. Shahbazi and H. Faraji, *Rev. Roum. Chim.*, **2020**, *65*, 291–303.

28. S. Özdemira, S. A. Mohamedsaid, E. Kılınçc and M. Soylak, *Food. Chem*., **2019**, *271*, 232–238.
29. A. Moghimi and M. Abniki, *J. Color Sci. Technol.*, **2022**, *15*, 301–315.
30. M. Abniki and A. Moghimi, *Micro & Nano Letters*, **2021**, *16*, 455–462.
31. A. Moghimi, M. Abniki, M. Khalaj and M. Qomi, *Rev. Roum. Chim.*, **2021**, *66*, 493–507.
32. R. Kalantari, A. Moghimi and F. Azizinezhad, *Rev. Roum. Chim*., **2021**, *66*, 895–906.
33. 32. A. Moghimi and M. Abniki, *Russ. J. Phys. Chem. B*, **2021**, *15*, S130–S139.
34. M. Abniki and A. Moghimi, *Curr. Anal. Chem.*, **2022**, *18*, 1070–1085.
35. K. Karimnezhad, A. Moghimi, R. Adnan and M. Abniki, *Micro & Nano Letters*, **2023**, *18*, e12150.
36. A. Moghimi, *Russ. J. Phys. Chem. A*, **2013**, *87*, 1203–1209.
37. M. Parsayi Arvand, A. Moghimi and M. Abniki, *IET Nanobiotechnology*, **2023**, *17*, 80–86.
38. M. Z. Manzoor, E. Yilmaz and M. Soylak, *Talanta*, **2017**, *174*, 645–651.
39. A. Moghimi, M. Qomi, M. Yari and M. Abniki, *Int. J. Bio-Inorg. Hybr. Nanomater.*, **2019**, *8*, 163–172.